

Fault Detection and Isolation in DFIG Driven by a Wind Turbine with a Variable Rotor Resistance

Hakim OUYESSAAD^a, Houcine CHAFOUK^a

^aIRSEEM – ESIGELEC, Technopole du Madrillet, Avenue Galilée, St Etienne du Rouvray 76801, France. E-mail address: hakim.ouyessaad@esigelec.fr & houcine.chafouk@esigelec.fr

Abstract : This paper presents a new approach to detect and isolate the current sensor faults, a doubly fed induction generator (DFIG) for a wind turbine application. And to detect the variable resistance faults. A method using an unknown input of multiple observers described via Takagi-Sugeno (T-S) multiple models. A bank of multiple observers scheme (DOS) generates a set of residuals for detection and isolation of sensor faults which can affect a TS model. A decision system is used to process the residual vector to detect and isolate faults. The stability and the performance of the multiple models are formulated in terms of Linear Matrix Inequalities (LMIs). The approach is validated using Matlab software to modeling and simulation of a DFIG.

Keyword: Wind Turbine; Current sensor Fault; parameter variation; Takagi-Sugeno Multiple models; Multiple Observer

1. Introduction

Since many wind turbines are installed at remote locations, the introduction of fault diagnosis and fault-tolerant control is considered a suitable way of improving reliability of wind turbine and lowering cost of repairs. As many wind turbines are installed earth and offshore, a non-planned service can be highly costly, so it would be beneficial if diagnosis could help the turbines to produce some energy from the time a fault is detected to the next planned service. A considerable research has been done on the modeling and control of wind turbines with DFIG [1,2,3]. Since monitoring the generator requires processing the current and measuring voltage, the first step should be dedicated to sensor fault diagnosis. That is why this issue is addressed here.

In this paper, complete diagnosis system for stator current, as well as rotor sensors are designed. Wind turbines have nonlinear aerodynamics and this limits the use of a linear equation. Hence, an increase in interest in diagnosis wind turbines through nonlinear methods has been noticed in the last years to handle the nonlinearity of the generator speed. This is achieved either through the use of nonlinear models directly in the design or through the use of multiple models approaches [4,5]. It is known that nonlinear unknown input observer design and diagnosis are difficult problems because powerful design methods are lacking to deal with nonlinearities. Unknown input observer design for general nonlinear systems is still largely a problem, and thus a nonlinear unknown input observer based on fault diagnosis remains an area for further research [6,7].

Recently several researchers have explored a Takagi-Sugeno (TS) fuzzy observer to deal with nonlinearity in problems detection and diagnosis. In [8] the authors proposed linear parameter-varying FTC systems for pitch actuator faults occurring in the full load operation. In [9] a T-S fuzzy observer based FTC design is proposed to achieve maximization of the power extraction. Other examples of this usage of the unknown input observers can be seen in [10] where the former reports similar schemes applied on fault detection of power plant coal mills and the latter estimate power coefficients for wind turbines, some examples can be found of fault detection and accommodation of wind turbines. An observer based scheme for detection of sensor faults for blade root torque sensor is presented in [11]. In [13] an unknown input observer based scheme was proposed to detect such faults in a wind turbine. The contribution of this paper focuses on the design of the unknown multiple observers to detect, isolate the current sensor faults and fault of variation resistance in the rotor circuit in DFIG, based on the wind turbine T-S models. This proposed scheme is based on the Dedicated Observers (DOS) method using a nonlinear unknown input observers scheme, each of the DOS is dedicated to each output of generator to generate a set of residual signals.

2. Modeling and observer design

The model is derived from the voltage equations of the stator and the rotor. It is assumed that the stator and the rotor windings are symmetrical and symmetrically fed. The saturation of the inductances, iron losses, skin effect, and bearing friction is neglected.

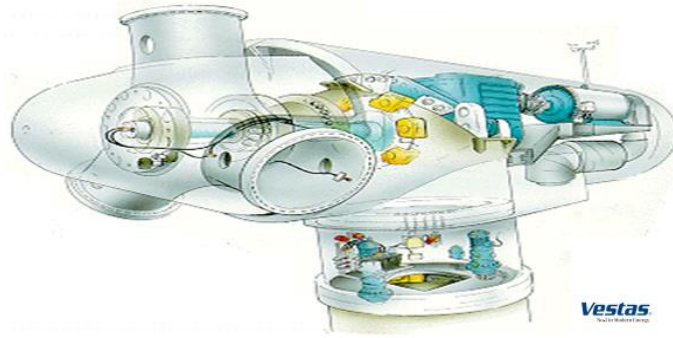


Figure. 1. Variable-speed wind system

The general state-space model is given in (1), (2) and (4), where $x(t)$ is the state system, $u(t)$ is the control vector input, $y(t)$ are measured and the output, $v(t)$ is the vector of unknown input. The matrices A , B , R and C are matrices known as the parameters of matrix which are defined in appendix, consistent with the dimension signals.

$$\dot{x}(t) = Ax(t) + Bu(t) + Rv(t), \quad y(t) = Cx(t) \quad (1)$$

$$u(t) = [V_{dr} \ V_{qr}]^T, \ v(t) = [V_{ds} \ V_{qs}]^T, \ x(t) = [i_{ds} \ i_{qs} \ i_{dr} \ i_{qr}]^T \quad (2)$$

$$\begin{cases} V_{ds} = R_s i_{ds} + \frac{d\phi_{ds}}{dt} - \omega_s \phi_{qs} \\ V_{dr} = R_r i_{dr} + \frac{d\phi_{dr}}{dt} - \omega_r \phi_{qr} \end{cases} \quad \begin{cases} V_{ds} = R_s i_{ds} + \frac{d\phi_{ds}}{dt} - \omega_s \phi_{qs} \\ V_{qs} = R_s i_{qs} + \frac{d\phi_{qs}}{dt} + \omega_s \phi_{ds} \end{cases} \quad (3)$$

where V stands for voltages (V), I stands for currents (A), R stands for resistors (Ω), ϕ stands for flux linkages (V.s). Indices d and q indicate direct and quadrature axis components, respectively, while s and r indicate stator and rotor quantities respectively. ω_s and ω_r are the stator and the (mechanical) rotor speed of the generator [12].

$$A = \begin{bmatrix} \frac{-R_s}{\sigma L_s} & p \left(\omega_s + \frac{L_h^2}{\sigma L_r L_s} \omega_r \right) & \frac{L_h R_r}{\sigma L_r L_s} & \frac{p L_h}{\sigma L_s} \omega_r \\ -p \left(\omega_s + \frac{L_h^2}{\sigma L_r L_s} \omega_r \right) & \frac{-R_s}{\sigma L_s} & \frac{p L_h}{\sigma L_s} \omega_r & \frac{L_h R_r}{\sigma L_r L_s} \\ \frac{L_h R_s}{\sigma L_r L_s} & \frac{-p L_h}{\sigma L_s} \omega_r & \frac{-R_r}{\sigma L_r} & p \left(\omega_s - \frac{\omega_r}{\sigma} \right) \\ \frac{p L_h}{\sigma L_r} \omega_r & \frac{L_h R_s}{\sigma L_r L_s} & -p \left(\omega_s - \frac{\omega_r}{\sigma} \right) & \frac{-R_r}{\sigma L_r} \end{bmatrix} \quad B = \begin{bmatrix} \frac{1}{\sigma L_s} & 0 \\ 0 & \frac{1}{\sigma L_s} \\ -\frac{L_h}{\sigma L_s L_r} & 0 \\ 0 & -\frac{L_h}{\sigma L_s L_r} \end{bmatrix} \quad R = \begin{bmatrix} -\frac{L_h}{\sigma L_s L_r} & 0 \\ 0 & -\frac{L_h}{\sigma L_s L_r} \\ \frac{1}{\sigma L_r} & 0 \\ 0 & \frac{1}{\sigma L_r} \end{bmatrix}$$

$$(\sigma) = 1 - \frac{L_h^2}{L_r L_s}: \text{ is the coefficient of Blondel} \quad (4)$$

Induction machines have a nonlinear nature, since the back EMF (electromotive force) depends on the rotational speed of the machine. This leads to a system matrix A that depends on the rotational speed, which is a variable (A is the nonlinear matrix) that is linear with respect to the states (e.g., currents) and also linear with respect to the rotational speed. The system matrices are explicitly given in (4), where ω_r is the mechanical rotor frequency, p is the number of pole pairs, and ω_A is the rotational frequency of the reference frame. Using this description, it is easily possible to convert the system from a stator fixed into a synchronous reference frame or onto any other frame, since the influence of the rotation is described by ω_A . Explicitly, a stator fixed system is using $\omega_A = 0$, while a system oriented with the stator's voltage uses the stator's angular frequency $\omega_A = \omega_s = 2\pi 50 \text{ s}^{-1}$. Moreover, the nonlinear models influences the rotor's mechanical speed ω_r - see Figure 2.

3. Obtaining multiple models

The multiple models represent nonlinear systems in the form of an interpolation between models in generally linear space premises. Each local model is a dynamic LTI (Linear Time Invariant) valid around an operating point. In a practical way, these models are obtained by identification, linearization around different various working points or by polytopic convex transformation. The interpolation of these local models using standard activation function is used to model global nonlinear systems. This approach, known as multiple models, is inspired by Takagi-Sugeno fuzzy models (T-S).

Takagi-Sugeno Multiple models

The structure of the Takagi-Sugeno model is the most widespread, both in the analysis and in the synthesis of the multiple models. The fuzzy models of T-S consist of set of rules. The global models are obtained by the aggregation of local models. It is expressed in the following form.

$$\begin{cases} \dot{x}(t) = \sum_{i=1}^r h_i(\xi(t)) (A_i x(t) + B_i u(t) + R v(t)) \\ y(t) = \sum_{i=1}^r h_i(\xi(t)) (C_i x(t)) \end{cases} \quad (5)$$

where r is the number of submodels, $\xi(t)$ is the measurable premise's variable, $h_i(\xi(t))$ are the membership functions verifying the convex sum's property $0 \leq h_i(\xi(t)) \leq 1$ and $\sum_{i=1}^r h_i(\xi(t)) = 1$, $x(t) \in \mathbb{R}^n$, $y(t) \in \mathbb{R}^p$ and $u(t) \in \mathbb{R}^m$ represent respectively the state, the output and input vectors $v(t)$ is the unknown input vector, $\{A_i, B_i, C_i, R\}$ are the sub models matrices.

Design of unknown input observers

In this section, we consider a nonlinear continuous time described by a multiple models, using activation functions that depend on the state of the system.

$$\begin{cases} \dot{z}(t) = \sum_{i=1}^r hi(\xi(t)) (N_i z(t) + G_i u(t) + L_i y(t)) \\ \hat{x}(t) = z(t) - Ey(t) \end{cases} \quad (6)$$

$N_i \in \mathbb{R}^{n \times n}$, $G_i \in \mathbb{R}^{n \times m}$, $L_i \in \mathbb{R}^{n \times p}$ is the gain of the i^{th} local observer, E is a transformation matrix.

Using the expression of $\hat{x}(t)$ given by (6) the expression of the error becomes:

$$e(t) = (I + EC)x(t) - z(t) \quad (7)$$

the time derivation of the estimation error is given by:

$$\begin{aligned} \dot{e}(t) = \sum_{i=1}^r hi(\xi(t)) (N_i e(t) + (PA_i - N_i P - L_i C)x(t) + (PB_i - G_i) u(t) \\ + PRv(t)) \end{aligned} \quad (8)$$

Solving Method

The method of resolution has been proposed to solve non-linear matrix inequalities and bilinear eq. [13].

$$(PA_i - K_i C)^T X + X(PA_i - K_i C) < 0 \quad \forall i \in \{1, \dots, r\} \quad (9)$$

we consider the following change of variable: $W_i = XK_i$ (10)

we consider the following Lyapunov function given by:

$$(PA_i)^T X + X(PA_i) - W_i C - C^T W_i^T < 0 \quad \forall i \in \{1, \dots, r\} \quad (11)$$

the solution of the inequality (11) can then be obtained using LMI conditions. For more information on the development of the method used to refer to [14,15].

4. Application to the diagnosis of the DFIG wind turbine

The multiple models (5) of the DFIG, in case of the presence of the faults current sensors. The different faults are modeled by an additional signal $f_c(t)$ in equation of measurement. The observed system becomes:

$$\begin{cases} \dot{x}(t) = \sum_{i=1}^r hi(\xi(t)) (A_i x(t) + B_i u(t) + Rv(t)) \\ y(t) = Cx(t) + D_c f_c(t) \end{cases} \quad (12)$$

where $f_c(t) = [f_{c1}(t) f_{c2}(t) f_{c3}(t) f_{c4}(t)]^T$ is the sensors fault vector, the non-linear models of the generator.

4.1. Simulation model of the generator

In order to assess the results of the simulation, we simulate two parallel models: multiple models and nonlinear models.

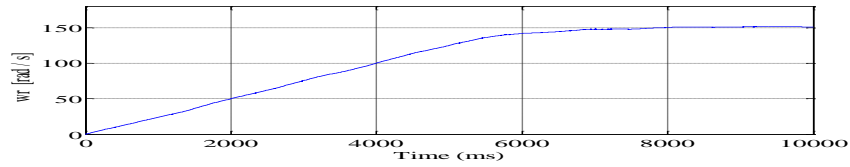


Figure. 2. The generator speed

The input applied is the same as that used for the non-linear models and the multiple models. Figure 3 show the superposition of the components of the vector output of the nonlinear models of the DFIG, and the approximation by multiple models.

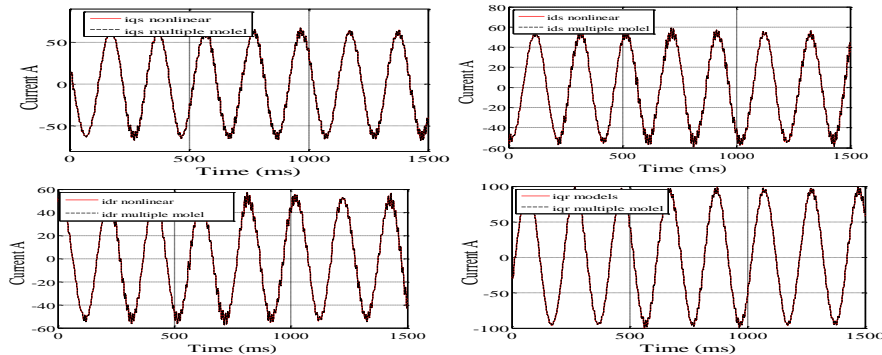


Figure.3. The output the non-linear model of DFIG and the multiple models estimation

The generation of residuals is a fundamental step in designing a diagnosis based on models. In theory, a residual should be zero in the absence of fault and significantly different from zero otherwise. It is then necessary to introduce detection thresholds to avoid false alarms.

4.2. Detection current sensors faults using DOS

The first scenario consists in introducing multiple faults in the outputs y_1 and y_4 . The fault is injected $f_1(t)$ and $f_4(t)$, at $t=0.189s$ and disappears $t=0.193s$. The fault consists of constant amplitude equal to 5% of the maximum amplitude of the output stator current I_{ds} and rotor current I_{qr} . The outputs $y_2(t)$ and $y_3(t)$ are assumed without. It should be noted that in the simulation a measurement noise is added to the output of the DFIG (here, a random signal with zero mean and variance equal to 1).

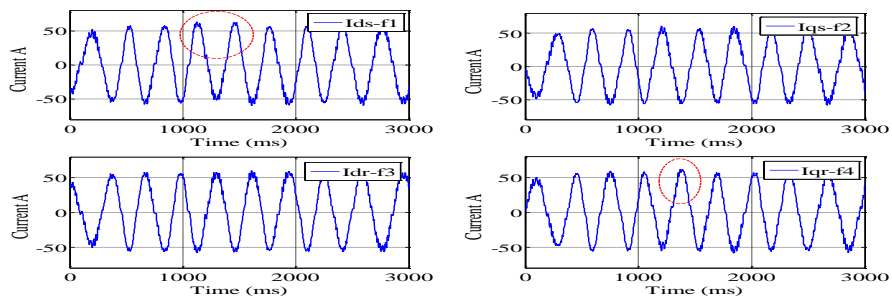


Figure. 4. Stator and rotor currents, the fault f_1 and f_4 in the current sensor

Using the DOS multiple observers, in this case, the i^{th} observer is controlled by the i^{th} output of the system as well as by all of the inputs. Figure 5 shows the architecture of the bank of DOS multiple observers.

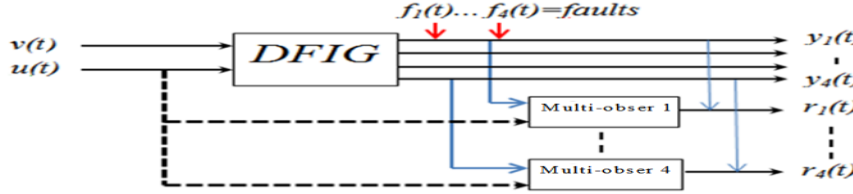


Figure. 5. Structure of multiple observer DOS

In this section, the detection of current sensor faults by the Luenberger multiple observers (5) will be focused on. The multiple observer 1 (DOS_1) reconstructs the models output using only the output y_1 , inputs $u(t)$ and unknown input $v(t)$ of the system. In this step the measurement y_1 is affected by a fault f_1 , and y_4 is affected by a fault f_4 . Fault f_1 is show during its presence in y_1 as is fault, f_4 in y_4 (red ellipse), as is show in Figure 4. Note that later $r_{DOSi,j}(t)$ is the fault indicator signal (residual), calculated from the difference between the j^{th} system output and the i^{th} estimated output, by the i^{th} DOS multiple observer. If the output has a fault, then there is a bad estimate of the state, and residual $r_{DOSi,j}(t)$ may be affected. The bench of DOS multiple observers enables us to generate different residuals with the presence of faults f_1 and f_4 $r_{DOS1}(t) = [1 \ 0 \ 0 \ 0]$, $r_{DOS2}(t) = [0 \ 1 \ 0 \ 0]$, $r_{DOS3}(t) = [0 \ 0 \ 1 \ 0]$ and $r_{DOS}(t) = [0 \ 0 \ 0 \ 1]$. From the results obtained it is found that the residuals r_{DOSii} are affirmative on the presence of faults of $y_1(t)$ and $y_4(t)$, as is show Figure 6.

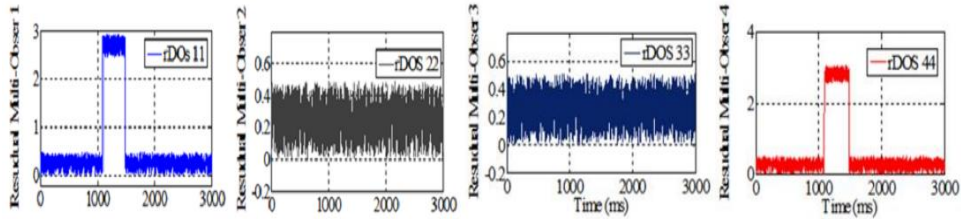


Figure. 6. Residual r_{DOS} obtained from DOS_i multiple observer

The multi observer DOS is capable to detect and isolate multiple and simultaneous faults.

5. Detection fault a variable rotor resistance

In order to validate the suggested diagnosis technique, acquisitions were performed using the variation of the rotor resistance of the generator. The choice of this parameter is explained by the various faults which affect the generator, which are apparent by a change due to temperature or a short circuit in the rotor and the stator. This observation was made in [16] and [17] where it was also found that the stator resistance R_s and R_r rotor are affected by the change of temperature operation for hot and cold tests. Here the variation in the initial values is around $\pm 30\%$ for both resistances. For a hot operation of the DFIG, the variation resistance is more important, with 30% for R_s and 20% for R_r .

The variations of the generator parameter are defined as system faults, which reflect a change in the parameters of the system. These faults can also be due to aging of the insulation resistance or saturation. It is obvious that the changes of resistance due to temperature are taken into account in the estimation procedure in the matrix A. This translates directly to the rotor and stator current in the DFIG generator. In [17] the author noted that the variation of the electrical parameters for a test concerns cold and hot

resistances. Temperature is the only parameter affecting resistances: a cold one will wake resistance decrease, where's a hot one will make then increase. In our study we specifically focus on the fault and the variation of the rotor resistance R_r .

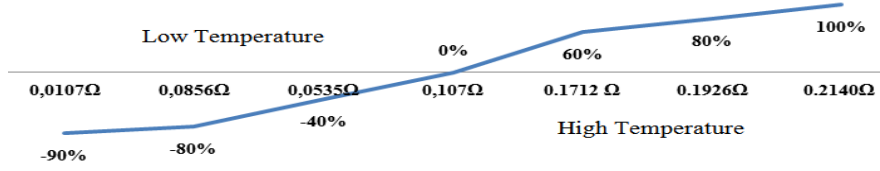


Figure. 7. Variable rotor resistance

5.1. Output error identification

We define the estimation error (residual identification noted r_{ids} and r_{idr} in the d -axis and the q -axis respectively) between the actual output for the nonlinear system (simulated currents i_{dqs}^* and i_{dqr}^*) and the output simulated by the (estimated) multiple models \hat{i}_{dqs} and \hat{i}_{dqr} by:

$$\text{for stator } \begin{pmatrix} r_{ids} = i_{ds}^* - \hat{i}_{ds} \\ r_{iqs} = i_{qs}^* - \hat{i}_{qs} \end{pmatrix}, \text{ for rotor } \begin{pmatrix} r_{idr} = i_{dr}^* - \hat{i}_{dr} \\ r_{iqr} = i_{qr}^* - \hat{i}_{qr} \end{pmatrix} \quad (13)$$

5.2. Analysis of residuals

For each residual $r_{ds}(t)$ and $r_{dr}(t)$, a tolerance τ (threshold) must be determined. The value of tolerance, is set according to the statistical characteristics of each residual in a system functioning normally. The tolerance value τ can, for example, be determined in this case compared to the current generator. For this type of generator tolerance not to exceed 3% and 5% of the nominal value (maximum current), to guarantee the proper functioning of the generator, and so as not to damage it. 0 or 1, that is affected or not by fault, is assigned to each residual. In simplified terms, the detection of faults in a residual is similar to the following logic test: if $|r_{ds,dr}| \leq \tau$ and $|r_{qs,qr}| \leq \tau$ then no faults can affects residuals, and if $|r_{ds,dr}| > \tau$ and $|r_{qs,qr}| > \tau$ then residuals are affected by a fault.

1st Case - Variation Δ_{R_r} (increase) of resistance R_r ; To see the behavior of the fault resistance on the rotor and stator generator operation, we propose to run a test in the presence of the rotor resistance variation. Table 1, shows the different cases for the simulation generator with an Δ_{R_r} variation (increase) of resistance R_r from 0% to 100% of its nominal value. In order to ensure a smooth functioning, only the expression of resistance in the rotor A matrix has been changed. The choice of the resistance variation of the values is very important, due to the comment previously mentioned, and then the application of the diagnosis method is used to detect faults of variation of resistance.

Table 1. Variation in the rotor resistance for operating at high temperature

Operating at high temperature	1 th case 0 %	2 nd case 60%	3 nd case 80%	4 nd case 100%
Δ_{R_r}	0 Ω	0.0642 Ω	0.0856 Ω	0.1070 Ω
R_r	0.1070 Ω	0.1712 Ω	0.1926 Ω	0.2140 Ω

Figure 7 shows the four currents of the rotor generator i_{dr} , obtained by the variation of the rotor resistance R_r following Table 1, use multiple model estimation

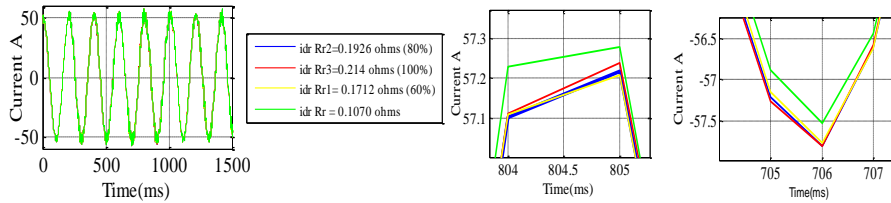


Fig. 7. Change in the rotor current due to change in the rotor resistance R_r (0% to 100%)

We note that the variation of rotor resistance produces a change in the rotor current i_{dr} , compared to the normal operation of the generator. As can be seen in the following figure, it represents the residuals for hot operation i.e. it corresponds to the increase in the rotor resistance. Figure 8 shows the evolution of residuals for different values of rotor resistance used, the residuals are obtained from the difference between the new rotor currents estimated by the multiple model obtained with the variation of the resistance R_r (0.1712 Ω , 0.1926 Ω and 0.2140 Ω) and the rotor current of the generator with $R_r = 0.1070 \Omega$. Close observation of Figure 9 it can be seen how the three residuals are relative to the change of the resistance R_r .

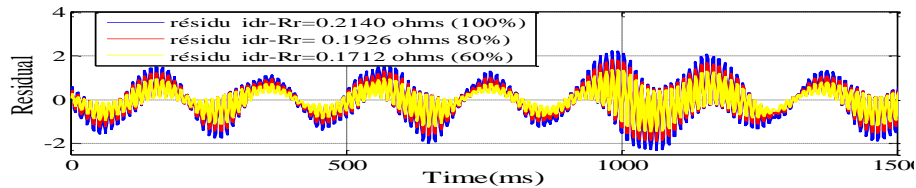


Figure 8. Evolution of residual signal with variation resistance R_r

We see that there is an important variation of residuals, when the rotor resistance exceeds 60% of the nominal value.

5.3. Decision system

Fault location is based on the comparison of the currents obtained for the system operation with the rotor resistance $R_r = 0.1070 \Omega$ (sane system) and operation with a variable resistance. In this part of the detection and isolation fault, we used values for the thresholds ($\tau = 3\%$ the maximum value of the current). The application of the detection test was applied to the residuals signals see Figure 8. Figure 9 shows the decision function of faults with the residual signals analysis, with $\tau = 3\%$.

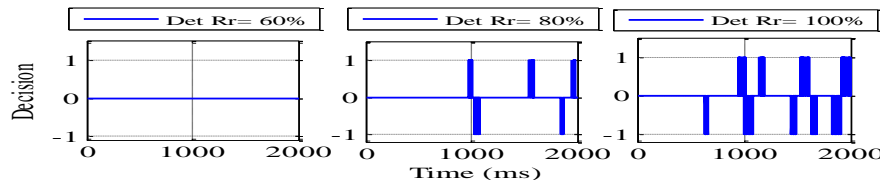


Figure 9. Detection and isolation faults

This part represents the influence of the rotor resistance variation on the currents rotor in the reference frame d (i_{dr}). It was found that the currents i_{qr} , i_{ds} and i_{qs} vary, this variation of

the current is due to the change (increase) of the value of resistor R_r between 0% and 100%. With the same reasoning as that applied to the current i_{dr} it detects the faults which affect the currents i_{qr} , i_{ds} and i_{qs} .

2nd Case - Variation Δ_{R_r} (decrease) of resistance R_r ; - see Table 2 and Figure 10. This last shows the different cases of simulation generator with Δ_{R_r} variation (decrease) resistance R_r 0% to -90% of its nominal value.

Table 2. Variation in the rotor resistance for operating at Low temperature

Operating at Low temperature	1 th case	2 nd case	3 rd case	4 th case
Δ_{R_r}	0 %	-40%	-80%	-90%
R_r	0.1070 Ω	0.0535 Ω	0.0214 Ω	0.0107 Ω

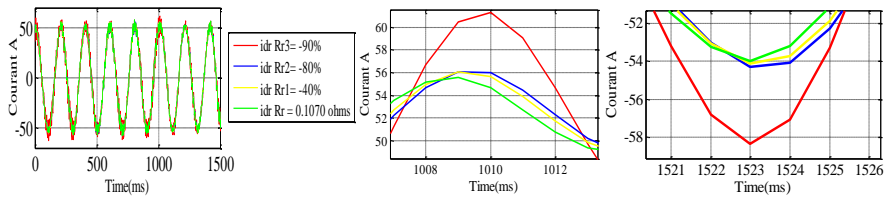


Figure 10. Change in the rotor current due to change in the rotor resistance R_r (0% to -90%)

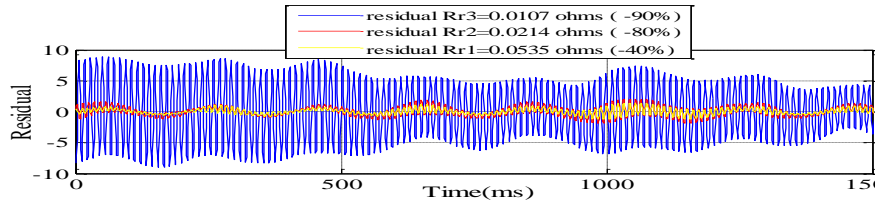


Figure 11. Evolution of residual signal with variation resistance R_r 0% to -90%

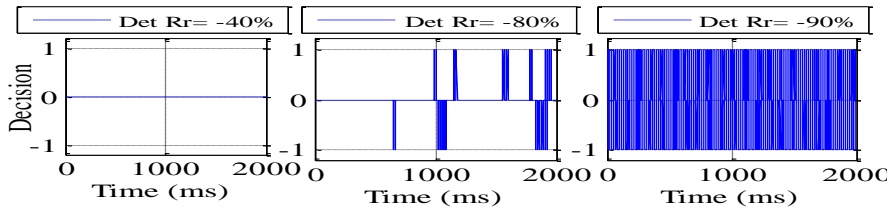


Figure 12. Detection and isolation faults for $\tau = 3\%$ (Low temperature)

It can be seen that, during the fault occurrence, the second component of $r_{idr} = 80\%$, $r_{idr} = -80\%$ and the third component $r_{idr} = 100\%$ and $r_{idr} = -90\%$. Both have mean values different from zero. This behavior corresponds to the one already presented in the paragraph (5), with respect to the threshold value. The fault is correctly detected and isolated, see Figure 9 and Figure 12. The fault is isolated within the required mean detection delay. In this section, we studied the influence of the rotor resistance of the rotor currents, similar results have been observed on other currents i_{qr} , i_{ds} and i_{qs} .

Conclusion

In this paper, the problem of current sensor and variable rotor resistance fault detection and isolation, for a DFIG driven by a wind turbine, has been addressed. An unknown input observer using TS models, was then used for state estimation and detection, isolation of

current sensor faults, which can affect nonlinear models. The approach has been validated using simulated signals of a double-fed induction generator for wind turbines. Through simulations, it has been demonstrated that multiple current sensor faults for rotor and stator have been correctly detected and isolated with a DOS. The future extension of this work lies in the control of a generator with a variation resistance in the rotor circuit of the machine.

Appendix

Parameters of the DFIG: Rated power (P) = 22 Kw, mutual inductance (L_h) = 45.8 mH, stator inductance (L_s) = 46.8 mH, rotor inductance (L_r) = 46.8 mH, stator resistor (R_s) = 0.1315 Ω , rotor resistor (R_r) = 0.1070 Ω , pairs of poles (p) = 2, [7].

References

1. Gálvez, C. Kinnaert, M. Sensor fault detection and isolation in doubly-fed induction generators accounting for parameter variations. *Renewable energy*, 36 1447e1457 (2011).
2. Odgaard, P. Thogersen, F. and Stoustrup, J. Fault isolation in parallel coupled wind turbine converters. *In Proceedings of European Wind Energy Conference 2009*. Marseille, France, (2009).
3. Chitti, B. Mohanty, K. B.. Doubly-Fed Induction Generator for Variable Speed Wind Energy Conversion. *Systems- Modeling & Simulation. International Journal of Computer and Electrical Engineering*, vol.2, no.1, pp.141-147, (2010).
4. Ostergaard, K. Stoustrup, J. and Brath, P. Linear parameter varying control of wind turbines covering both partial load and full load conditions. *International Journal of Robust and Nonlinear Control*, 19, 92-116, (2009).
5. Lescher, F. Zhao, J.-Y. and Borne, P. Switching LPV Controllers for a Variable Speed Pitch Regulated Wind Turbine. *International Journal of Computers, Communications and Control*, Vol.I pp. 73-84, (2006).
6. Trinh, D. Chafouk, H. Fault diagnosis and isolation using kalman filter bank for a wind turbine generator. *IEEE/MED Conference CORFU.*, Greece (2011).
7. Rothenhagen, K. Thomsen, S. and Fuchs, F. W. Doubly fed induction generator model-based sensor fault detection and control loop reconfiguration. *IEEE on industrial electronics*, vol. 56, no. 10, pp. 4229–4238, (2009).
8. Kamal, E. Koutb, M, Sobaih, A and Abozalam, B. An intelligent maximum power extraction algorithm for hybrid wind-diesel-storage system. *Int. J. Electr. Power Energy Syst.*, vol. 32, pp. 170-177, 2010.
9. Kamal, E. Aitouche, A, Ghorbani, R. and Bayart, M. Unknown Input Observer with Fuzzy Fault Tolerant Control for Wind Energy .*IFAC SAFEPROCESS 2012*. August 29-31, 2012.Mexico.pp 946-951, (2012)
10. Odgaard, P.F. Stoustrup, J. Unknown input observer based scheme for detecting faults in a wind turbine converter. *In proceedings of the 7th IFAC symposium on fault detection, supervision and safety of technical processes*, page 161–166, Barcelona, Spain, (2009).
11. Wei, X. Verhaegen, M and Van-Den-Engelen, T. Sensor fault diagnosis of wind turbines for fault tolerant. *In Proceedings of the 17th World Congress The International Federation of Automatic*, Seoul, South Korea, pp.3222–3227, (2008).
12. Sejir, Khojet EL-Khail, and al. Rotor flux oriented control of a doubly fed induction machine. *International Power Electronics and Motion Control Conference, EPE-PEMC 2004*, September 1-4, Riga, Latvia, (2004).
13. Ouyessaad, H. Chafouk, H and Lefebvre, D. Doubly fed induction generator fault diagnosis using unknown input Takagi-Sugeno observer. *Control, Decision and Information Techenologie, CODiT*, May 6-8 at Hammamet, Tunisia, (2013).
14. Bourar, T. and al. Robuste non-quadratic static output feedback controller designe for Takagi-Sugeno systems uning descriptor redundancy. *Elsevier, Engineering Application Intelligence*, 26(2): 739-756, Februry (2013).
15. Ouyessaad, H. Chafouk, H. Unknown input observer for detecting current sensor faults for a DFIG in wind turbine. *Integration modeling and analysis applied control and automation, IMAACA 2012*, Vienne. Autriche, September (2012).
16. Bachir, S. Contribution au Diagnostic de La machine Asynchrone par Estimation Paramétrique. *Thesis (PhD)*, University of Poitiers, France (2002).
17. Esbensen, T.S and Slot, C. Fault Diagnosis and Fault-Tolerant Control of Wind Turbines. Master's thesis, Faculty of Engineering, Section for automation and control, Aalborg University- Danmark. June 3rd (2009).